



## Broadband imaging, least-squares migration in the image domain, and depth-domain inversion over a production field in the Mississippi Canyon area, Gulf of Mexico

Mohamed Hegazy\*, Leo Leon, Mohamed Sabri Majdoub, Olga Zdraveva, and Charles Inyang, WesternGeco; Ken Hargrove, Ridgewood Energy; Katy Pasch and John Hollins, LLOG Exploration

Copyright 2019, SBGf - Sociedade Brasileira de Geofísica

This paper was prepared for presentation during the 16<sup>th</sup> International Congress of the Brazilian Geophysical Society held in Rio de Janeiro, Brazil, 19-22 August 2019.

Contents of this paper were reviewed by the Technical Committee of the 16<sup>th</sup> International Congress of the Brazilian Geophysical Society and do not necessarily represent any position of the SBGf, its officers or members. Electronic reproduction or storage of any part of this paper for commercial purposes without the written consent of the Brazilian Geophysical Society is prohibited.

### Abstract

Starting a new acquisition program can be difficult due to the current challenging market conditions; however, maximizing the value of preexisting seismic data through applying modern technologies can provide a faster and cheaper solution. Customizing a workflow for specific imaging challenges and interpretation objectives can achieve significant image improvement over the legacy volumes with an affordable cost.

This case study illustrates superior imaging results over legacy volumes through a successfully integrated broadband and amplitude-friendly reprocessing workflow that incorporated adaptive noise attenuation, adaptive deghosting, and a multidimensional, beyond-aliasing interpolation. An effective model building workflow was executed in parallel with signal processing to provide an on-time imaging solution that was critical to support drilling plans. In addition, a novel amplitude-friendly post-migration image enhancement was deployed to ensure improved resolution and interpretability, even in areas of limited illumination.

Complex geology and limitations imposed by the surface seismic acquisition geometry often result in seismic images contaminated by the variable illumination effects. To mitigate these effects and to achieve a higher-resolution image of the reservoir, represented by thin subsalt sand beds, we used least-squares migration in the image domain. Furthermore, we demonstrate the results from a depth-domain inversion workflow using point-spread functions.

The reprocessed image shows significant improvement over the legacy data in terms of bandwidth, resolution, signal-to-noise ratio, structural continuity, amplitude fidelity and overall image interpretability. The chosen overall imaging strategy yielded high-quality inversion results and enabled critical drilling decisions.

### Introduction

Understanding amplitude plays is important as seismic amplitudes are often used successfully as direct hydrocarbon indicators (DHI) for supra-salt sand reservoirs. As the focus of future exploration and production in the deep-water Gulf of Mexico (GoM) moves

to deeper subsalt amplitude plays, understanding subsalt amplitude anomalies has become vital. Unfortunately, the presence of salt bodies can create variable illumination patterns imprinted on subsalt images and distort the true seismic amplitudes. Therefore, it is very important to model and remove the variable illumination effects to reveal the true rock properties embedded in the seismic image.

The Mississippi Canyon area, located in the northeastern GoM, is characterized by extensive allochthonous salt canopies that cause poor subsalt illumination, affecting severely the quality of seismic images and reliability of the inversion products. The target prospect under investigation is represented by several relatively thin sand intervals, totaling approximately 200-300 ft of thickness and located just below the base of salt.

There are several wells in the area and, based on similarities in amplitude behaviour, new potential drilling targets were identified. The new imaging exercise goal was to provide better understanding of and insight into the viability of existing and new targets.

Data used in this case study were obtained from a wide-azimuth (Corcoran et al., 2007) survey acquired in 2008 and 2009, with an 8-km maximum offset. The current reprocessing scope commenced from navigation-merged shot records. An initial evaluation of the available data was conducted to understand the challenges that must be addressed to help de-risk the image interpretability in this area. The key challenges identified included:

- 1) Poor subsalt image resolution, insufficient to understand and preserve the subsalt amplitudes.
- 2) Sparse crossline sampling.
- 3) Significant seismic well misties, up to 350 ft, hence, a low-confidence legacy velocity model.
- 4) Poor subsalt image interpretability due to salt model uncertainty, signal-to-noise ratio, and acquisition limitations.
- 5) Illumination-related amplitude variations.

To address these challenges and achieve the project objectives, we designed a reprocessing and imaging strategy executed in four main stages and incorporated several advanced techniques.

- 1) Signal processing: This included noise attenuation, adaptive deghosting (Rickett et al., 2014), multiple attenuation, and prestack 3D matching-pursuit Fourier interpolation (Schonewille et al., 2013).
- 2) Earth model building: This involved supra-salt common image point (CIP) tomography (Woodward et al., 2008), salt interpretation, localized seismic imaging (O'Brian et al., 2013) utilizing reverse time migration (RTM) vector

image partitions (VIP) (Cogan and Boochoon, 2013), and subsalt CIP tomography using RTM subsurface angle azimuth gathers.

- 3) Image conditioning and enhancement: This is comprised of dip-guided selective stacking (Gu et al., 2018), illumination-driven image optimization, and interpretation-guided image enhancement (Gu et al., 2016).
- 4) Least-squares migration in the image domain (LSM-i) (Fletcher et al., 2016) and depth-domain inversion (DDI) (Fletcher et al., 2012).

The reprocessing effort resulted in a more-accurate earth model, higher-resolution images that compensated for variable illumination amplitudes, and reliable inversion products for prospect development plans.

### 3D deghosting and demultiple

Adaptive deghosting (AD) uses sparse decomposition in the local plane-wave domain in tau-p space and computes the delay for both the 3D source and receiver ghosts simultaneously. Deghosting was essential to recover the low-frequency signal normally attenuated by marine ghost effects. In addition, deghosting enabled a better definition of steeply dipping events as shown in Figure 1.

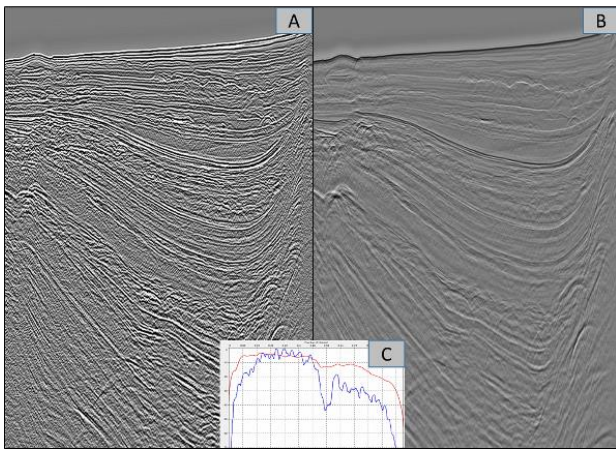


**Figure 1** - Stacked section in open basin: A) before AD, B) after AD, C) amplitude spectrum, blue: before AD, red: after AD.

The AD process was applied prior to multiple prediction to enhance the low-frequency multiples for accurate multiple modeling and effective multiples attenuation across the seismic bandwidth.

### Model building – supra-salt tomography

Even though the starting earth model was detailed and mature, a mis-tie of up to 210 ft was observed at the top-of-salt well marker. Thus, revisiting the supra-salt velocity was vital to minimize depth errors at the targets.

Adjustment of anisotropic parameters, followed by one iteration of multiazimuth CIP tomography with Kirchhoff depth migration (KDM) gathers produced a geologically plausible model update that yielded a better image and improved gather flatness, as well as a reduction of the mis-tie to 20 ft at the top-of-salt marker (Figure 2).

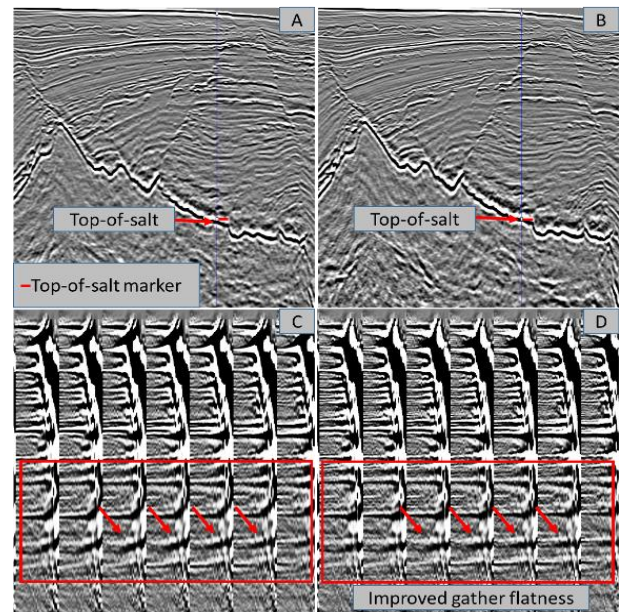


**Figure 2** - Broadband KDM image through well location: A) before CIP tomography with up to a 210-ft mis-tie, B) after CIP tomography with reduced mis-tie. KDM gathers at the well location, C) before CIP tomography showing non-flat gathers, and D) after CIP tomography with improved gather flatness

### Localized seismic imaging

Localized seismic imaging (LSI) is an interpretation-driven workflow in which targeted modifications are made to a baseline velocity model and the impacts are quickly evaluated on either RTM or KDM migrated images (O'Briain et al., 2013). LSI involves processing targeted subsets of data, typically around the areas of interest. For this study, three areas of interest were identified and a total of ten LSI iterations were performed. The LSI work was focused on:

- 1- Sediment velocity inclusions inside the salt and velocity scans.
- 2- Overhang zones refinement to better delineate the regional base-of-salt horizon.
- 3- Incorporating missing salt wings in two areas of interest (Figures 3A and B).

Due to the complexity of salt canopies, it was vital to use RTM vector image partitions to reveal hidden information (Figure 3D) and enable a more accurate salt geometry interpretation.

### Illumination-driven image optimization

Subsalt imaging can be challenging in areas of poor illumination. Selecting only shots contributing to the illumination of a given target horizon and migrating the selected shots only can provide significant uplift to the image interpretability (Hartman et al., 2015).



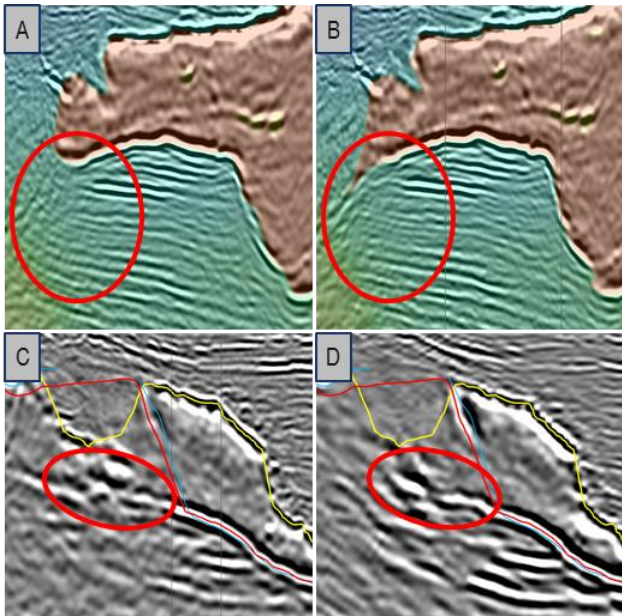


**Figure 3** - RTM image before A), and after incorporating a salt wing B). Red oval shows less migration noise after model improvement by adding more salt. RTM salt-flood full image C), and partial image using selected VIPs D). Red ovals show better base-of-salt continuity as a result of stacking VIP tiles that image the base-of-salt only

An illumination-driven image optimization (IDIO) technique was utilized to resolve subsalt imaging at an area of interest in the presence of a thrust-fault zone that suffered from low illumination and an extensive amount of noise. Two conflicting steeply dipping horizons were identified and used to isolate the corresponding shots that contribute to the illumination. To overcome the challenge, ray-tracing illumination (RTI) studies were performed on both target horizons separately to isolate the shots contributing to each horizon. The selected shots for each horizon were migrated separately to generate RTM VIPs. A simple stacking post migration showed significant uplift to the image interpretability (Figure 4). The produced VIPs from the IDIO process were utilized for the final image enhancement in addition to providing higher weights to the signal and relatively suppressing the noise.

Figure 5 shows the accumulated effect of the described techniques included in the customized workflow. It is evident that the new reprocessing effort yielded an improved model and, correspondingly, an image with improved resolution, events continuity, and general interpretability.

#### Least-squares migration in the image domain

The key input to performing LSM-i or DDI is a grid of point-spread functions (PSFs). The PSFs grid is a representation of the spatially variant 3D wavelet embedded in the migrated image and it captures the dip- and space-dependent illumination effects due to acquisition geometry and complex geology (Letki et al., 2015).

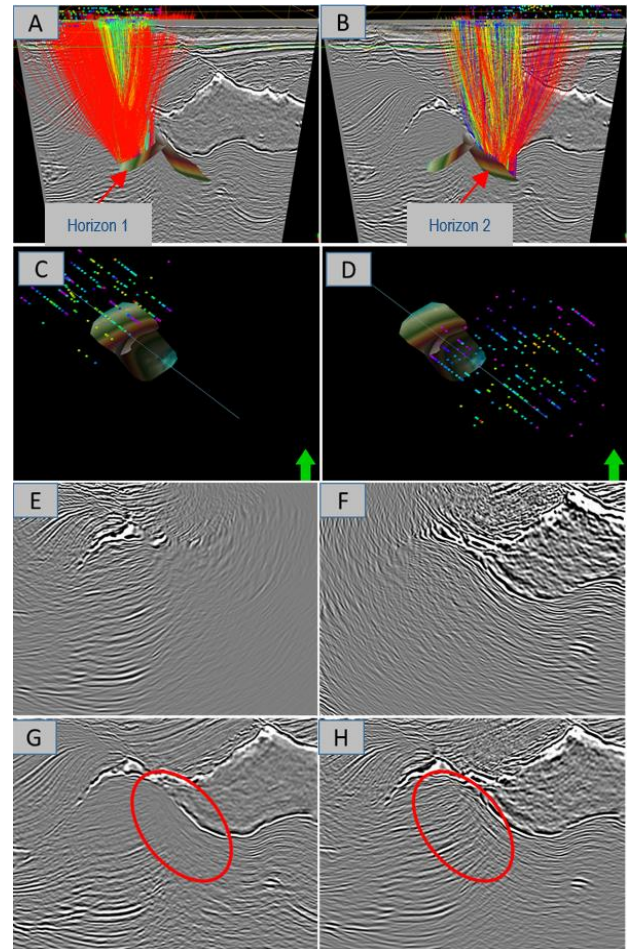


**Figure 4** - A) RTI successful rays over Horizon 1, B) RTI successful rays over Horizon 2, C) selected shot locations for Horizon 1, and D) selected shots locations for Horizon 2. E) Migration result using selected shots from Horizon 1, and F) migration result using selected shots from Horizon 2, G) all shots migration at the area of interest red oval shows the noise completely masking the target, and H) sum of selected shots migrations for Horizons 1 and 2. Red oval shows where the image is significantly improved.

Because illumination effects are related to acquisition limitations and geology complexity, PSFs were generated using the true data acquisition geometry and best available earth model. Using a constant reflectivity target horizon convolved with the information captured in the PSFs, the modeled illumination variability expected at the target horizon was obtained. A root-mean-square (RMS) amplitude extraction of the RTM image migrated with the same earth model was also performed along the target horizon (Figure 6). Comparisons between the forward-modeled illumination imprints along the target horizon and the RMS amplitude of the RTM image demonstrated high correlation and proved that illumination imprints on the subsalt seismic amplitudes exist.



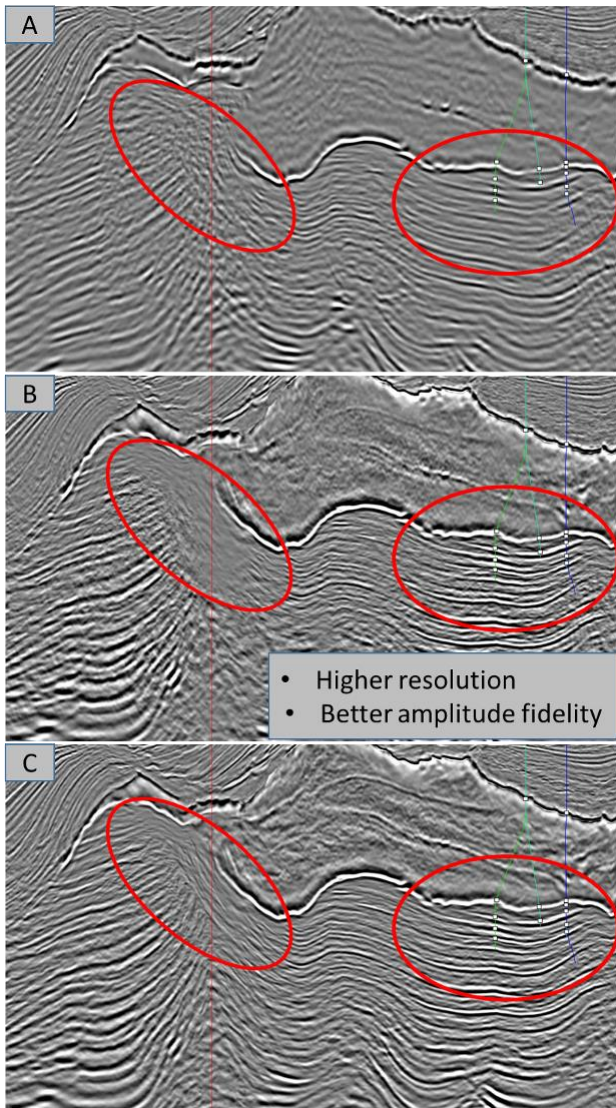


**Figure 5** - RTM images: A) enhanced legacy image; the red ovals show the low resolution at target and the poor continuity at subsalt targets. B) Raw reprocessed image; there is an overall significant improvement. Also, the right red oval shows the higher-resolution data, the amplitude fidelity preservation achieved by broadband processing, and the improved model building. C) Final enhanced reprocessed image; there is an overall improved structure as well as improved subsalt continuity.

LSM-i allows us to retrieve the underlying subsurface pseudo-reflectivity by modelling and removing illumination effects imprinted on the migrated image. It requires no well information. Because the PSFs capture (1) the 3D depth- and-space-variant wavelet and, hence, distortion effects in the imaging system, and (2) dip- and depth-dependent illumination information, they can be used to iteratively deconvolve the conventional RTM image. The result is a higher-resolution image, free of illumination imprints, allowing more reliable amplitude mapping (Figures 7 and 8).

A key assumption with any least-squares migration is that the seismic data have been kinematically imaged correctly.

If the earth model is suboptimal, LSM-i or DDI will not be able to compensate for the model errors. LSM-i and DDI will correct for 3D wavelet variations due to illumination; however, they will not correct for wavelet variations due to inaccurate imaging.

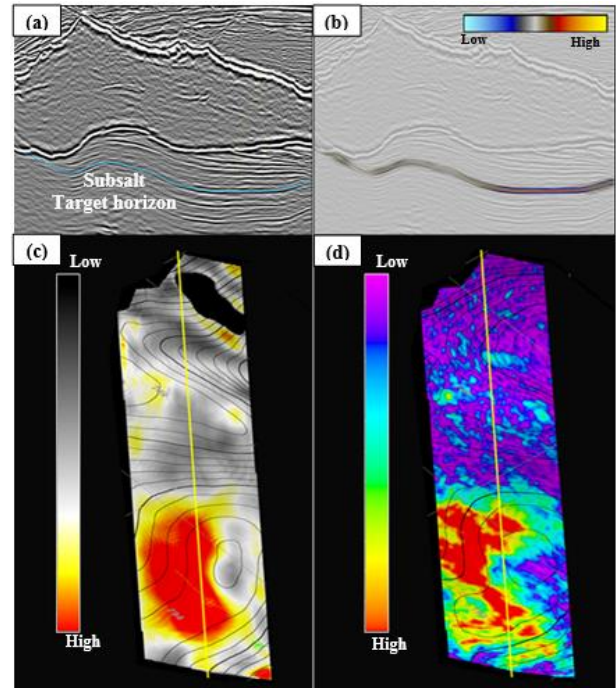


**Figure 6** - (a) RTM image with subsalt target horizon overlaid, and (b) modeled illumination response for the given earth model and acquisition geometry. Areal map displays of target horizon showing (c) modeled illumination response captured by PSFs, and (d) RMS amplitude extracted from the seismic data. High illumination correlates with high RMS subsalt amplitudes.

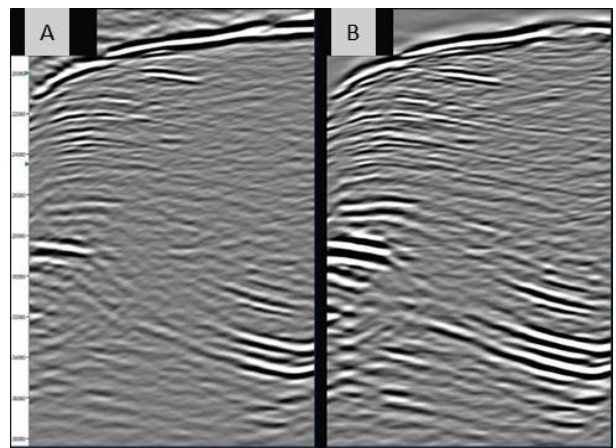


**Figure 7** - (A) Conventional 30-Hz RTM image, (B) LSM-i showing improvement in the continuity of subsalt events.

In this study, a reverse time migration modelling engine was used to generate our point-spread functions. RTM-PSFs are generated with spacing versus cost tradeoffs. At high contrasts in the migration velocity model, the PSF variation across such discontinuities can be severe, most

noticeably in the wavelet stretch and in differing dips illuminated (Fletcher et al., 2018). Addressing this salt boundary imprint on the PSFs was vital prior to conducting LSM-i or DDI in this project (Leon et al., 2018). It ensured preservation of the amplitude fidelity just below the base of salt where the targets lie.

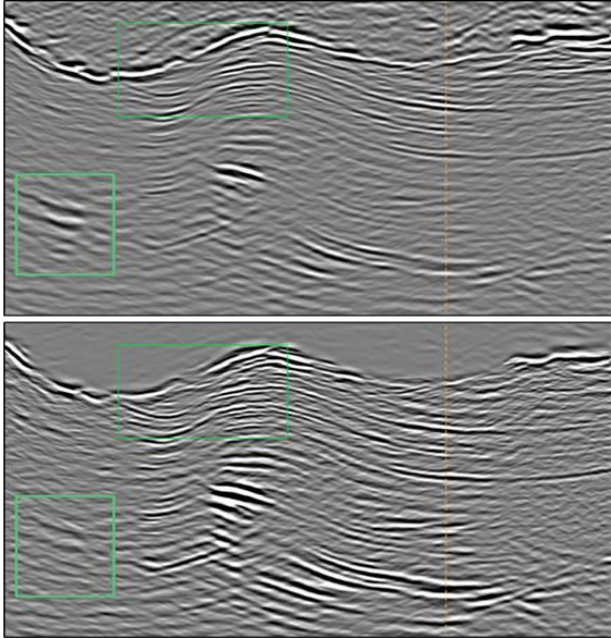


**Figure 8** - (a) Conventional 30-Hz RTM image, (b) LSM-i showing (upper box) no distortion in the image close to the salt-sediment boundary, and (lower box) improvement in the resolution of subsalt events as a correction for over-fold illumination. In general, more consistent amplitudes are visible across each geological horizon.

### Depth-domain inversion

The DDI workflow is an extension of LSM-i. DDI inverts the depth-migrated seismic data in the depth domain using 3D depth- and space-variant wavelets (PSFs) to capture and correct for space- and dip-dependent illumination effects resulting from acquisition geometry and complex geology. The output includes a reflectivity image corrected for illumination effects and an absolute acoustic impedance (AI) volume. The DDI workflow utilized the following inputs: reverse time migration seismic data, a grid of well-calibrated 3D PSFs, dip fields for optional preconditioning that helps mitigate boosting of noise, and an AI low-frequency model. The inversion is carried out in depth and, therefore, does not require multiple domain conversion of the depth-migrated seismic image.

From the 3D convolution of reflectivity (derived from the acoustic impedance low-frequency model) with the calibrated 3D PSFs, synthetic seismic data are created for comparison with the input seismic data and the residual (difference between seismic and synthetic data) is calculated. The model is then updated by minimizing an objective function to derive the model with an image that best fits the data (Fletcher et al., 2012). A key step in depth-domain inversion is the seismic well ties and residual

wavelet extraction for PSF calibration, which is required to obtain a true reflectivity volume. The inversion to derive absolute acoustic impedance requires low-frequency data missing in the seismic bandwidth. The seismic frequency spectrum is estimated to determine the missing frequencies and the low-frequency model is generated from filtered acoustic impedance logs with seismic migration velocity used as a guide model.

Results from applying this workflow are summarized in Figure 9, showing the input RTM seismic image with annotated subsalt hydrocarbon targets and brine-saturated interval. The RTM image amplitudes do not truly represent the reservoir and non-reservoir intervals for the thin sands (labeled 1, 2, 3, and 4 in Figure 8) due to the acquisition limitations and geology complexity and must be correctly estimated. The reflectivity volumes from LSM-i (Figure 8B) and DDI (Figure 8C) show a more balanced amplitude that is representative of the fluid content (brine and hydrocarbon) at the sand intervals. The DDI reflectivity image shows an improved resolution compared to the input seismic data and LSM-i reflectivity due to the PSF calibration. Figure 8D shows the equivalent output acoustic impedance volume with hydrocarbon targets and brine-saturated interval.

### Conclusions

This case study illustrates superior imaging results relative to a good legacy product through a successfully integrated amplitude-friendly broadband signal processing workflow as well as an efficient, parallel model building strategy and a wide variety of post-image enhancement techniques. Least-squares migration in the image domain simultaneously provides a higher-resolution image of thin subsalt sands while correcting for illumination effects. The reflectivity image and acoustic impedance volumes yielded by depth-domain inversion allowed interpreters to discriminate between hydrocarbon and brine-saturated sands and augment their prospect development plans.

### Acknowledgements

We thank Ridgewood Energy and LLOG Exploration for permission to jointly publish this case study. We thank WesternGeco Multiclient and TGS for permission to show the legacy data. We also thank Alexander Zarkhidze, Emil Nassif, Sherman Yang, Michael O'Briain, Robin Fletcher, Sherif Guirguis, and Lei Zhang for their contributions to this work.

### References

- COGAN, M., AND BOOCHOON, S. Sub-salt seismic interpretation using RTM vector image partitions: 83rd Annual International Meeting, SEG, Expanded Abstracts, 1338-1342, 2013.
- CORCORAN, C., PERKINS, C., LEE, D., CATTERMOLLE, P., COOK, R., AND MOLDOVEANU, N. A wide-azimuth streamer acquisition pilot project in the Gulf of Mexico: The Leading Edge, 26(4), 460-468, 2007.



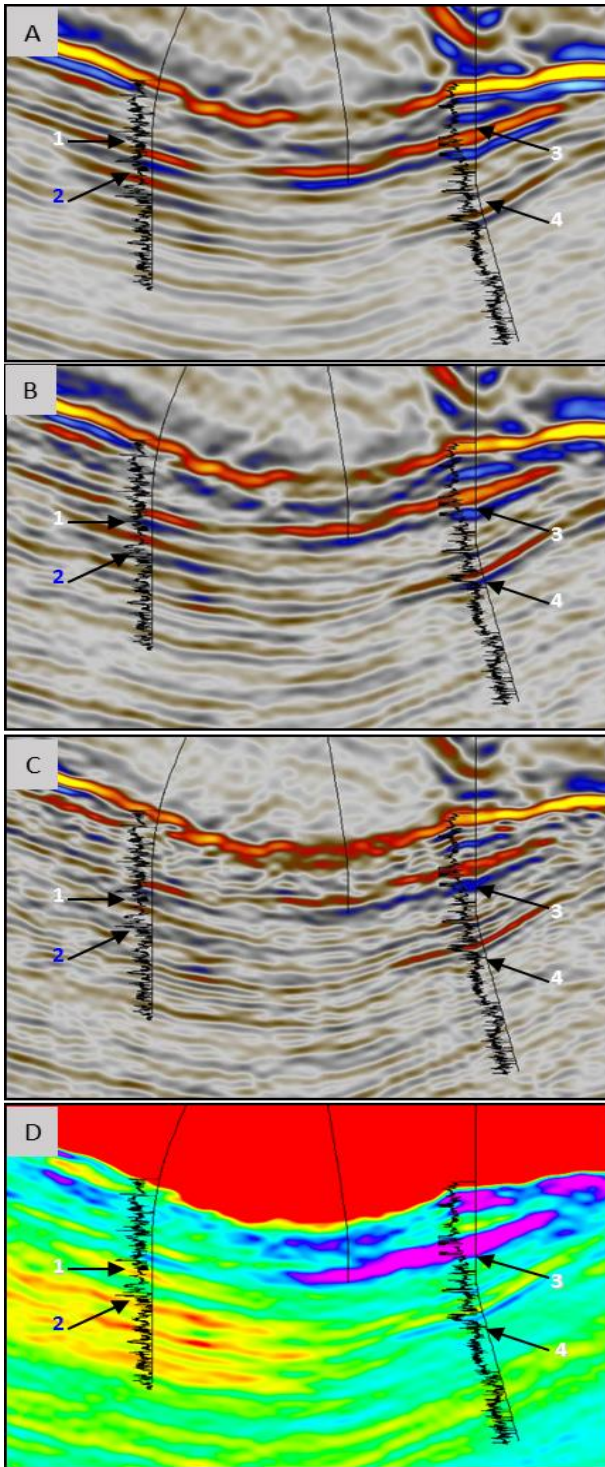


**Figure 9** - (A) Conventional RTM image, (B) LSM-pseudo-reflectivity image, (C) DDI reflectivity image, and (D) inverted acoustic impedance volume. 1, 3, and 4 (hydrocarbon), and 2 (brine) sands

FLETCHER, R., CAVALCA, M., AND NICHOLS, D. Improving image-domain least-squares reverse-time migration close to high velocity contrasts: 80th Conference and Exhibition, EAGE, Extended Abstracts, 2018.

FLETCHER, R.P., ARCHER, S.H., NICHOLS, D., AND MAO, W. Inversion after depth imaging: 82nd Annual International Meeting, SEG, Expanded Abstracts, 1-5, 2012.

FLETCHER, R. P., NICHOLS, D., BLOOR, R. AND COATES, R.T. Least-squares migration - Data domain versus image domain using point spread functions, TLE, 2016.

GU, R., ZDRAVEVA, O., HEGAZY, M., AND BUZZELL S. Interpretation Guided Image Enhancement using RTM Vector Image Partitions: 78th EAGE Conference and Exhibition, Extended Abstracts, 2016.

GU, R., HEGAZY, M., AND ZDRAVEVA O. Geologic Structure-based Image Enhancement with Directional Image Partitions: 80th EAGE Conference and Exhibition, Extended Abstracts, 2018.

HARTMAN, K., CHAKRABORTY, S., NOLTE, B., GOU, W., SUN, Q., AND CHAZALNOEL, N. Understanding and improving the subsalt image at Thunder Horse, Gulf of Mexico: 85th Annual International meeting, SEG, Expanded Abstracts, 4028-4032, 2015.

LEON, L., INYANG, C., HEGAZY, M., HYDAL, S., HARGROVE, K., PASCH, K., AND HOLLINS, J. Least-squares migration in the image-domain and depth-domain inversion: A Gulf of Mexico case study. SEG Technical Program Expanded Abstracts, 4146-4150, 2018.

LETKI, L., TANG, J., AND XIANG, D. Depth Domain Inversion a Case Study in Complex Subsalt Area: 77th Conference and Exhibition, EAGE, Extended Abstracts, 2015.

O'BRIAIN, M., SMITH, D., MONTOYA, C., BURGESS, B., KOZA, S., ZDRAVEVA, O., ISHAK, M., ALWON, S., KING, R., NIKOLENKO, D., AND VAUTIER, S. Improved subsalt imaging and salt interpretation by RTM scenario testing and image partitioning: 83rd Annual International Meeting, SEG, Expanded Abstracts, 3856-3860, 2013.

RICKETT, J., VAN MANEN, D.-J., LOGANATHAN, P., AND SEYMOUR, N. Slanted-streamer data-adaptive deghosting with local plane waves: 76th EAGE Conference and Exhibition, Extended Abstracts, 2014.

SCHONEWILLE, M., YAN, Z., BAYLY, M., AND BISLEY, R. Matching pursuit Fourier interpolation using priors derived from a second data set: 83rd Annual International Meeting, SEG, Expanded Abstracts, 3651-3655' 2013.

WOODWARD, M., NICHOLS, D., ZDRAVEVA, O., WHITFIELD, P., AND JOHNS, T. A decade of tomography, Geophysics, 73, 5-11, 2008.